Catalysis Science & Technology

Effect of Alkali Metal Addition on Catalytic Performance of $Ag/ZrO_2/SBA-16$ Catalyst for Single-Step Conversion of Ethanol to Butadiene

Journal:	*Catalysis Science & Technology*
Manuscript ID	CY-ART-10-2022-001722.R1
Article Type:	Paper
Date Submitted by the Author:	29-Nov-2022
Complete List of Authors:	Winkelman, Austin; Washington State University Voiland College of Engineering and Architecture, Chemical Engineering and Bioengineering; Pacific Northwest National Laboratory, Dagle, Vanessa; Pacific Northwest National Laboratory, Lemmon, Teresa; PNNL, Kovarik, Libor; Pacific Northwest National Laboratory, EMSL Wang, Yong; Pacific Northwest National Laboratory, Institute for Integrated Catalysis; Washington State University, Voiland School of Chemical Engineering and Bioengineering Dagle, Robert; Pacific Northwest National Laboratory,

Effect of Alkali Metal Addition on Catalytic Performance of $Ag/ZrO_2/SBA-16$ Catalyst for Single-Step Conversion of Ethanol to Butadiene

Austin D. Winkelman[1,2], Vanessa Lebarbier Dagle[1*], Teresa L. Lemmon[1], Libor Kovarik[1,3], Yong Wang[1,2], Robert A. Dagle[1*]

[1] *Institute for Integrated Catalysis, Pacific Northwest National Laboratory, 902 Battelle Blvd., Richland WA 99354 USA*
[2] *Voiland School of Chemical Engineering and Bioengineering, Washington State University, Pullman WA 99163 USA*
[3] *Environmental Molecular Sciences Laboratory, Pacific Northwest National Laboratory, Richland WA 99354 USA*

For submission to:

Catalysis Science & Technology

*Corresponding Authors

Email address: vanessa.dagle@pnnl.gov, robert.dagle@pnnl.gov

Abstract

This paper describes how adding Na and K to a 4Ag/4ZrO_2/SBA-16 catalyst enhances catalytic performance for single-bed conversion of ethanol to butadiene. While adding Na and K leads to a slight decrease in conversion (i.e., ~10% loss), the production of desired butadiene is significantly increased with up to 50% improvement in productivity for the 4Ag/4ZrO_2/SBA-16 catalyst promoted with 0.5% Na. The reasons for this improvement are a beneficial decrease in Lewis acid site concentration and higher Ag dispersion when Na or K are added, which results in decreased activity involving ethanol dehydration to ethylene and diethyl ether. A remarkable butadiene selectivity of 75% was achieved while maintaining high conversion (i.e., 90%) with 0.5Na/4Ag/4ZrO_2/SBA-16 catalyst. A 72-hour catalyst lifetime study shows that because of higher coke formation from polymerization of desired butadiene, catalyst deactivation occurs more rapidly with the 0.5Na/4Ag/4ZrO_2/SBA-16 (55% loss in conversion) than with 4Ag/4ZrO_2/SBA-16 (45% loss in conversion). However, this does not alter the advantageous effect of Na addition because the butadiene yield remained higher throughout the study period for 0.5Na/4Ag/4ZrO_2/SBA-16. A key finding is that during the reaction, Na limits sintering of Ag particles and promotes selective coking of the acid sites responsible for ethylene and diethyl ether formation.

1.0 Introduction

As a precursor in the production of a wide range of significant synthetic elastomers and copolymer plastic products, butadiene is one of the most high-value and high-volume compounds used in the chemical industry. Its current annual global demand is approximately 1.2 billion MT,(1) and with projected market growth of its use in the automobile industry and the manufacture of copolymers, worldwide market demand for butadiene has been forecasted to reach USD $23.49 billion by 2027.(2) More than 95% of the butadiene currently used is a co-product of C_4 crude fractions separated downstream of steam crackers that produce ethylene. Traditionally, feedstocks for ethylene crackers have been heavier gasoil (in North America) and naphtha-based slates (in Europe). Over the last decade, increasing shale gas production rates from fracking have caused ethylene crackers to move toward the use of lighter feedstocks, and inexpensive, gas-derived ethane is becoming the preferred feedstock of North American cracker operations. In Europe, feedstocks are shifting from naphtha to lighter butane and propane feedstocks. This is a substantial problem for butadiene production as heavier cracker feedstocks produce far more crude C_4 fractions than light cracker fractions, so much so that most light cracker fractionation operations do not have butadiene separation units.(3) Without an alternative means of production, the supply of butadiene is expected to decrease in the future.

Over the past several decades the use of biofuels in the transportation sector has been promoted to facilitate energy independence and lessen the environmental impact of fossil fuel use. This has led to ethanol becoming the predominant biofuel produced worldwide. There are several sustainable routes to ethanol production for use as a platform molecule in its catalytic upgrading to value-added products. Three factors have been identified that will likely lead to competitively priced, plentiful ethanol in the near future: 1) production beyond the ethanol “blend wall” that

limits its use as a transportation fuel, 2) advances to production efficiency, and 3) diversification of process feedstocks (i.e., deployment of syngas and waste gas fermentation processes at scale in addition to the traditionally used corn glucose or sucrose feedstocks).(4) In 2019, approximately 54% of the world's 29 billion gallons of fermentation-based ethanol production originated in the United States,(5) placing it in a good position to benefit from an advantageous market to use ethanol as a platform molecule for the production of industrially relevant bulk chemicals that traditionally have been derived from oil. Of the potential chemicals that can be formed from ethanol over mixed metal oxide catalysts, butadiene is one of the highest-value products to be considered. Butadiene was once produced from ethanol at industrial scale before the process fell out of favor economically in the 20th century when the conventional cracking method became preferred. Butadiene was produced either directly from ethanol via the one-step Lebedev process(6) or via the two-step Ostromisslensky process using a mixture of co-fed ethanol and acetaldehyde.(7) Over the last 20 years, interest in the conversion of ethanol to butadiene has increased significantly, and many challenges have presented themselves regarding process intensification and catalyst viability due to the complexity of the cascade of reactions that take place and the need to minimize the formation of the many possible reaction side-products.(8, 9) The development of a large-scale, coproduct-independent butadiene process is a greatly sought-after goal, and an optimized ethanol-to-butadiene process has the potential to be a renewable means to achieve that goal.

Recently, we reported a highly active $Ag/ZrO_2/SiO_2$ catalytic system for one-step production of butadiene.(10) For silica-supported Ag and ZrO_2 ethanol-to-butadiene catalysts, several papers in the last decade have been published examining each of the generally accepted mechanism steps using proposed intermediates as reactants over ethanol-to-butadiene catalysts in addition to kinetic

and characterization studies. These studies provide conclusions suggesting it is reasonable to assume that the Toussaint's aldol condensation mechanism is occurring over the system.(11-14) Figure 1 shows the generally accepted mechanism for the five-step ethanol-to-butadiene reaction.

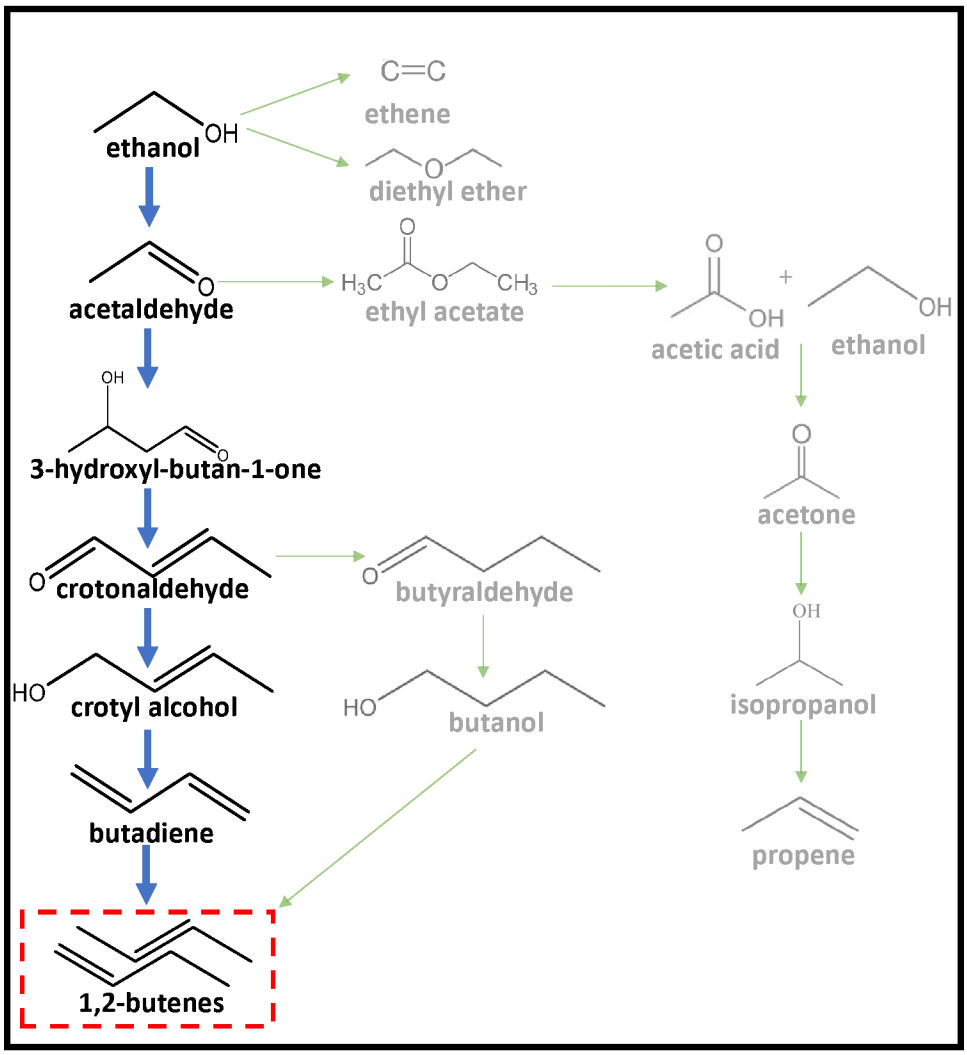

Figure 1 Generally accepted mechanism for the ethanol-to-butadiene reaction (*in black*) with relevant side reactions and products (*in grey*). Adapted from Makshina et al.(15)

In step 1, ethanol is first dehydrogenated to acetaldehyde. In step 2, two acetaldehyde molecules undergo aldol condensation to form 3-hydroxybutanal. In step 3, the 3-hydroxybutanal is dehydrated to form crotonaldehyde. In step 4, a Meerwin-Ponndorf-Verley (MPV) reduction step occurs with ethanol as the proton donor to form crotyl alcohol and acetaldehyde. Finally, in

step 5, 1,3-butadiene is formed via subsequent dehydration. Then, 1,3-butadiene may undergo partial hydrogenation to 1,2-butenes. For the Ag/ZrO_2/SBA-16 system, Ag sites were found to be responsible for ethanol dehydrogenation to acetaldehyde and the ZrO_2/SiO_2 provides the needed Lewis acid sites for further conversion of acetaldehyde to butadiene in the aldol condensation and MPV reduction steps. A key finding was a correlation between overall Lewis acid site concentration and selectivity to butadiene.(10)The dehydration steps are facile compared to the other reactions steps and are believed to occur over weak acid sites present on surfaces of SiO_2 or ZrO_2.(15)

In this study, we examined the effect of the addition of the alkali metals Na and K on the catalytic performance of 4Ag/4ZrO_2/SBA-16 (baseline) catalyst in relationship with the catalysts properties. Because the Lewis acid sites and the Ag metal are the active sites for butadiene production from ethanol, the catalysts were characterized using pyridine adsorption followed by Fourier transform infrared resonance (FTIR) spectroscopy, high-resolution transmission electron microscopy (HRTEM), and X-ray diffraction (XRD) analysis before and after reaction. Evaluation of catalyst activity over lifetimes of 72 hr time-on-stream (TOS) also were carried out for the baseline 4Ag/4ZrO_2/SBA-16 and the preferred 0.5Na/4Ag/4ZrO_2/SBA-16 catalyst.

2.0 Experimental Details

2.1 Catalyst Synthesis

The series of xM/yAg/zZrO_2/SiO_2 catalysts were synthesized by incipient wetness impregnation of SiO_2 (SBA-16 from ACS Materials) with $AgNO_3$ powder (Sigma Aldrich), and $ZrO(NO_3)_2$ solution (Sigma Aldrich) dissolved in deionized water. For the catalyst systems with alkali metals, $NaNO_3$, or KNO_3 (Sigma Aldrich) were mixed with the solution of $AgNO_3$ and $ZrO(NO_3)_2$ in deionized water before impregnation. The values x, y, and z correspond to catalyst

loading in wt.%. After incipient wetness impregnation, the catalysts were dried at 110°C for 8 hr and calcined at 500°C for 4 hr.

2.2 Catalyst Characterization

2.2.1 Pyridine Adsorption/Desorption Followed by Infrared Spectroscopy

Acidity measurements were conducted using a Nicolet FTIR spectrometer IS50 equipped with a mercury cadmium telluride detector (resolution: 4 cm^{-1}, 128 scans) to record infrared spectra. All spectra presented in this manuscript were normalized for 100 mg of the catalyst. Samples were pressed into pellets (ca. 20 mg for a 2-cm^2 pellet), and a pellet was placed inside the transmission infrared cell. Samples were pretreated at 400ºC under N_2 for 2 hr and then under 10% H_2/N_2 at 325ºC for 1 hr before final cooling to 50ºC. After pretreatment, pyridine was introduced at 50ºC ($P_{equilibrium}$ = 133 Pa), and the spectra were recorded following desorption from 50 to 350ºC. The number of Lewis acid sites titrated by pyridine was calculated using an integrated molar absorption coefficient value of ε = 2.22 $cm.\mu mol^{-1}$ for ν_{19b} vibration of coordinated pyridine at approximately 1450 cm^{-1}.(16) For experiments involving catalyst exposure to ethanol, the catalyst was pretreated under ultrahigh vacuum at 400°C for 2 hr after the initial Py-IR experiment before being exposed to ethanol at 4 Pa at 325°C. The cell then was returned to ultra-high-vacuum conditions before the second set of Py-IR desorption spectra were acquired.

2.2.2 Total Carbon Analysis

Total carbon analysis to determine the amount of solid carbon deposited on the spent catalysts during lifetime studies were measured by a Shimadzu Total Carbon Analyzer (TOC-5000A using an SSM-5000A Solid Sample Module). Three separate measurements were taken for each sample and their results were averaged for the presented data.

2.2.3 X-Ray Powder Diffraction

X-ray diffraction patterns were recorded using a Philips X'pert MPD (Model PW3040/00) diffractometer with a copper anode (Kα1 = 0.15405nm) and a scanning rate of 0.0013° per second between 2θ = 10° to 90°. Jade 5 (Materials Data Inc., Livermore, CA) and the Powder Diffraction File database (International Center for Diffraction Data, Newtown Square, PA) were used to analyze the diffraction patterns. The catalysts were reduced at 325°C for 1 hr under 5% H_2/N_2 prior to this analysis.

2.2.4 Scanning Transmission Electron Microscopy

Transmission electron microscopy images were obtained using an FEI Titan 80-300 at 300kV. Images were digitally recorded with a charge-coupled device camera and subsequently analyzed using the Gatan DigitalMicrograph® software suite. Briefly, sample preparation involved mounting powder samples onto copper grids covered with lacey carbon support films before directly loading them into the TEM airlock to minimize exposure to atmospheric O_2. The samples were reduced at 325°C for 1 hr in 10% H_2/N_2 before imaging. At least 10 different locations on the grid were used to collect TEM images. A sample size of over 200 particles was used in this analysis to determine the Ag° particle size of each catalyst.

2.3 Reactivity Measurements

Reactivity tests for the conversion of ethanol to butadiene were carried out in a 9.53-mm outer diameter (8.64-mm inner diameter) fixed-bed, packed-bed reactor loaded with 2.0 g of catalyst. A K-type thermocouple was inserted into the reactor to measure the temperature of the catalyst bed. An electrical resistance heating block was installed on the reactor to minimize the development of temperature gradients, and a temperature feedback loop with proportional-integral-derivative control was used to maintain constant bed temperature during the reaction. Catalysts first were

activated in situ prior to testing at 450°C for 8 hr under 100 sccm N_2 before cooling to the reaction temperature of 325°C. The catalyst then was reduced under 100 sccm of 5% H_2/N_2 for 1 hr. Liquid feed was introduced to the system using an ISCO syringe pump, and a vaporizer heated to 120°C (consisting of 8.64-mm inner diameter steel tubing filled with quartz beads) was used to convert reactants to the gas phase before reaching the reactor. Conversion and selectivity of the catalyst were measured at 325°C. Carbon-based ethanol conversion and selectivities were calculated using equations (1) and (2).

$$\text{Ethanol Conversion (\%)} = \frac{\text{moles of C (in ethanol)in} - \text{moles of C (in ethanol)out}}{\text{moles of C in}} \times 100 \quad (1)$$

$$\text{Carbon Selectivity to x (\%)} = \frac{\text{moles of C in x}}{\text{moles of total C in product}} \times 100 \quad (2)$$

where x is a product formed in the reaction. The reactor pressure was equal to 1 atmosphere for all experiments and the ethanol partial pressure was equal to 11% (balance N_2). The weight hourly space velocity (WHSV) of ethanol was between 0.23-0.31 hr^{-1} as noted in tables description. A back pressure regulator was placed directly downstream of the reaction zone followed by a knockout pot cooled to 5°C to collect liquid product. Gaseous effluent from the reactor was analyzed online using an Inficon micro-GC (Model 3000A) equipped with MS-5 A, Plot U, alumina, OV-1 columns, and a thermal conductivity detector. Liquid samples from the knockout pot were collected and analyzed separately ex situ using liquid chromatography.

3.0 Results and Discussion

3.1 Effect of Alkali Metals on Catalytic Performance

We previously demonstrated that butadiene selectivity is directly related to the concentration of Lewis acid sites for single-bed conversion of ethanol to butadiene over $Ag/ZrO_2/SiO_2$ catalysts.(10) While acid sites are needed to allow aldol condensation of acetaldehyde, a high concentration of acid sites is undesirable. Indeed, acid-catalyzed reactions, such as ethanol

dehydration to ethylene and diethyl ether (DEE) are favored as the concentration of acid sites increases, resulting in lower butadiene selectivity. Several studies have shown that addition of alkali metals to mixed oxides catalysts helps improve selectivity to butadiene by minimizing formation of side-reaction products such as ethylene and DEE.(17, 18)·(19) Therefore, we assessed the impact that Na and K alkali metals have on the catalytic performance of the $4Ag/4ZrO_2$/SBA-16 catalyst. The results presented in Table 1 show that under the same reaction conditions (T = 325°C, P = 1 atmosphere, WHSV= 0.23 hr^{-1}), adding Na or K leads to about 10% loss in conversion. At similar conversion levels (i.e., 86–90%), adding Na or K to the baseline $4Ag/4ZrO_2$/SBA-16 catalyst results in a significant decrease in ethylene and DEE selectivity, especially for the catalyst with Na addition for which ethylene and DEE selectivities are 5× and 8× lower, respectively. This is accompanied by an increase of butadiene selectivity as follows: 52.7% for $4Ag/4ZrO_2$/SBA-16, to 61.7% for $0.5K/4Ag/4ZrO_2$/SBA-16, and to 75.1% for $0.5Na/4Ag/4ZrO_2$/SBA-16. As a result, butadiene productivity is 50% higher for the $0.5Na/4Ag/4ZrO_2$/SBA-16 catalyst and equal to 0.12 g butadiene/g catalyst/hr. Note that under optimal reaction conditions, a high butadiene productivity equal to 0.4 g butadiene/g catalyst/hr was achieved with the baseline catalyst (See Table S1). Thus, butadiene productivity greater than 0.4 potentially could be achieved when Na is added under improved reaction conditions. Separately, the selectivity to alkanes is one magnitude higher for the $0.5K/4Ag/4ZrO_2$/SBA-16 catalyst (i.e., 7.7%) compared to the baseline catalyst (i.e., 0.2%). This improved selectivity may be attributed to structural and electronic effects on the favorability of alkene hydrogenation activity of Ag on the catalyst surface after K addition.(20, 21)

Table 1. Effect of Na and K addition to 4Ag/4ZrO_2/SBA-16 baseline catalyst on ethanol-to-butadiene activity.

Catalyst	WHSV (hr^{-1})	Conversion (%)	Selectivity (%)									Productivity*
			Ethylene	DEE	Acetaldehyde	Propylene	Butenes	Butadiene	Pentenes	C2–C5 Alkanes	Other Oxygenates	
4Ag/4ZrO_2/SBA-16	0.23	95.8	8.3	7.6	2.5	1.7	7.9	67.9	0.6	0.8	2.4	0.09
4Ag/4ZrO_2/SBA-16	0.31	86.4	14.6	14.8	7.7	2.6	6.1	52.7	0.0	0.2	1.2	0.08
0.5K/4Ag/4ZrO_2/SBA-16	0.23	86.6	4.5	3.9	8.1	2.3	8.2	61.7	0.7	7.7	2.6	0.1
0.5Na/4Ag/4ZrO_2/SBA-16	0.23	89.8	3.3	1.8	2.1	1.8	10.2	75.1	0.8	1.0	3.3	0.12

P_{EtOH}= 11% ethanol/balance N_2. P = 1 atmosphere. T = 325°C.
Other oxygenates included ethyl acetate, butanol, acetone, crotonaldehyde, crotyl alcohol.
* grams butadiene per gram of catalyst and per hour

.

Overall, the results show that both Na and K positively affect the catalytic performance because formation of desired butadiene is increased and production of undesired ethylene and DEE is diminished. To understand this behavior the catalyst active sites were measured by pyridine followed by FTIR for acidity quantification and HRTEM for Ag particle size determination.

Figure 2 presents the FTIR spectra obtained after pyridine adsorption at 50°C followed by desorption at 150°C for all three catalysts.

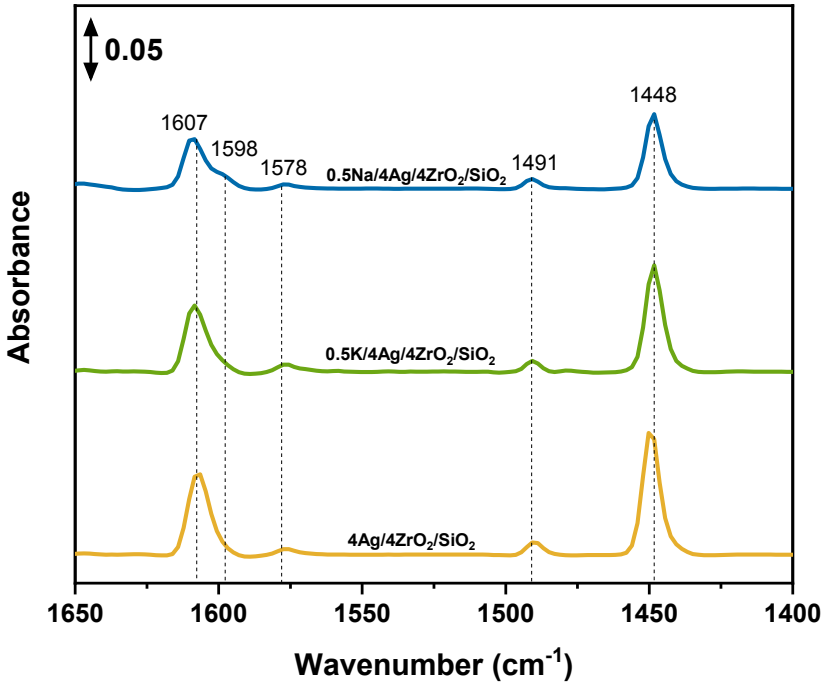

Figure 2. Infrared spectra recorded after pyridine adsorption at 50°C followed by desorption at 150°C for the alkali metal on $Ag/4ZrO_2/SBA\text{-}16$ and baseline catalysts (the baseline spectra recorded prior to pyridine adsorption were subtracted from the ones obtained after pyridine desorption at 150°C). Spectra were normalized to a pellet of 20 mg and 2 cm^2. Py-L at 1448 cm^{-1} was used for quantification.

As reported in previous investigations of $Ag/ZrO_2/SiO_2$ catalysts, only bands characteristic of Lewis acid sites are detected (i.e., no Brønsted acid sites were observed in the spectra).(10), (22) The concentration of the Lewis acid sites reported in Table 2 is highest for the baseline catalyst (i.e., 43.4 µmoles/g) and lowest for the $0.5Na/4Ag/4ZrO_2/SBA\text{-}16$ catalyst (i.e., 25.5 µmoles/g).

Table 2. Ag particle size and Lewis acid site concentrations for 0.5K/4Ag/4ZrO_2/SBA-16, 0.5Na/4Ag/4ZrO_2/SBA-16 and the baseline 4Ag/4ZrO_2/SBA-16. Average Ag particle sizes were calculated from TEM images, and acid site concentrations were determined by desorption of pyridine followed by FTIR at 150°C (weak), 250°C (medium), and 350°C (strong).

Catalyst	Average Ag Particle Size (nm)	Lewis Acid Site Concentration (μmol/g)			
		Weak	Medium	Strong	Total
4Ag/4ZrO_2/SBA-16	2.7	35.1	7.2	1.1	43.4
0.5K/4Ag/4ZrO_2/SBA-16	2.2	26.1	3.1	7.0	36.2
0.5Na/4Ag/4ZrO_2/SBA-16	1.9	20.6	3.4	1.4	25.5

Thus, addition of Na and K to the 4Ag/4ZrO_2/SBA-16 catalyst neutralizes some of the Lewis acid sites limiting the conversion of ethanol to ethylene and DEE dehydration products and favors the ethanol dehydrogenation pathway ultimately leading to butadiene formation. Accordingly, these results can explain, at least in part, the decrease in dehydration product (i.e., ethylene and DEE) selectivity and increase in butadiene selectivity upon addition of Na and K.

Ag particle size for the three fresh catalysts was determined by HRTEM. Representative images are shown in Figs. S2–S9, and relative statistics and particle size distributions are shown in Figs. S10–S12. Table 2 shows that the Ag particle size decreases upon addition of alkali metals from 2.7 nm for the baseline catalyst to 2.2 nm and 1.9 nm for the catalysts with 0.5K/4Ag/4ZrO_2/SBA-16 and 0.5Na/4Ag/4ZrO_2/SBA-16, respectively.

One possible explanation is that Na and K interact with Ag during synthesis, thereby limiting aggregation of Ag species leading to higher Ag metal dispersion in the resulting catalyst. Here, the 0.5Na/4Ag/4ZrO_2/SBA-16 catalyst with the smallest Ag particles presents the lowest dehydration products selectivity, and the 4Ag/4ZrO_2/SBA-16 catalyst with the larger Ag particles presents the highest dehydration products selectivity. This added information is interesting, as in our previous work, we found that formation of ethanol dehydration products (i.e., ethylene and DEE) is favored with larger Ag particles.(23) Hence, we can conclude that both Na and K help decrease the

formation of ethylene and DEE in favor of butadiene production due to lower concentration of acid sites and lower Ag particles size of the fresh catalysts.

Figure 3 shows the evolution of the butadiene selectivity (a) and dehydration product (i.e., ethylene and DEE) selectivity (b) as a function of Lewis acid site concentrations for the three catalysts from this study (labeled as 0.5M/4Ag/4ZrO_2/SBA-16) and for two other Ag/ZrO_2/SiO_2 catalyst series included in our previous work.(10)

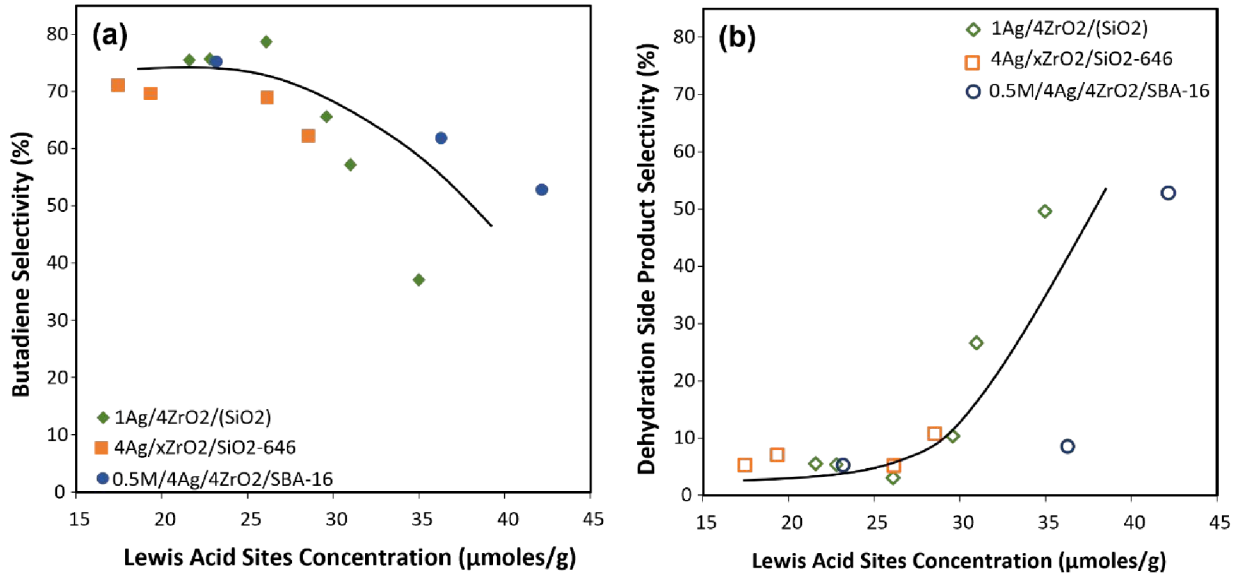

Figure 3. (a) Evolution of butadiene selectivity and (b) dehydration side-product selectivity at 75–90% ethanol conversion with the total concentration of Lewis acid sites determined after pyridine desorption at 150°C for the 1Ag/4ZrO_2/(SiO_2) series on various silica supports, the 4Ag/xZrO_2/SiO_2-646 series of increasing ZrO_2 loadings supported on Davisil 646 (both from previous work(10)), and 0.5M/4Ag/4ZrO_2/SBA-16 catalysts from this work. M corresponds to each alkali metal investigated. Solid symbols correspond to butadiene selectivity, and open symbols represent dehydration product selectivity.

In general for all the catalyst series studied, butadiene selectivity decreases and dehydration product selectivity increases when the concentration of Lewis acid sites increases. Lewis acidity is shown to be necessary for aldol condensation of acetaldehyde molecules and MPV reduction of

crotonaldehyde with ethanol in the reaction mechanism; however, excess acidity leads to an increase in ethanol dehydration activity that results in a decrease in butadiene selectivity.

Given that higher butadiene selectivity was achieved with 0.5Na/4Ag/4ZrO_2/SBA-16 (75.1%), this catalyst was selected for additional stability studies in comparison with the baseline 4Ag/4ZrO_2/SBA-16 catalyst.

3.2 Effect of Na Addition on the Catalyst Lifetime of 4Ag/4ZrO_2/SBA-16

Catalyst stability has been a long-standing challenge for single-step conversion of ethanol to butadiene. Catalysts typically deactivate quickly because of coking from butadiene polymerization.(24) Here, we investigated catalyst lifetimes for the baseline 4Ag/4ZrO_2/SBA-16 catalyst and the more promising 0.5Na/4Ag/4ZrO_2/SBA-16 catalyst. Figure 4 illustrates ethanol conversions and selectivities to butadiene and the dehydration side-products diethyl ether and ethylene with respect to time one stream for both catalysts.

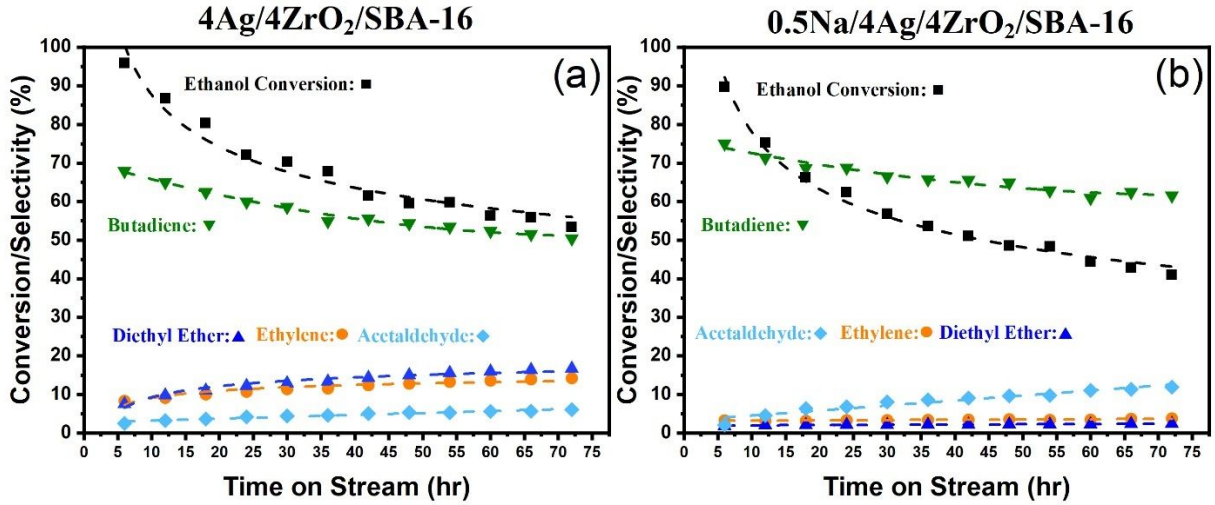

Figure 4. Effect of Na addition on baseline catalyst activity and deactivation. a) 4Ag/4ZrO_2/SBA-16 lifetime and b) 0.5Na/4Ag/4ZrO_2/SBA-16 lifetime. $WHSV_{EtOH}$ = 0.23 hr^{-1}. P_{EtOH} = 11% in N_2. P = 1 atmosphere. T= 325°C. Selectivity details can be found in Tables S2 and S3.

While both catalysts suffer from deactivation, the loss of conversion does not occur instantly as often observed for this reaction. Also, the initial conversion (TOS = 5 hr) is only slightly lower for 0.5Na/4Ag/4ZrO_2/SBA-16 (i.e.,90%) compared to 4Ag/4ZrO_2/SBA-16 (i.e., 96%). However, after 72 hr TOS, the decrease in conversion becomes more significant for 0.5Na/4Ag/4ZrO_2/SBA-16 (i.e., 41%) compared to 4Ag/4ZrO_2/SBA-16 (i.e., 53%). This decrease is attributed to a more rapid coking of the active sites over the 0.5Na/4Ag/4ZrO_2/SBA-16 catalyst. Indeed, the total carbon analysis results presented in Table S2 show a greater presence of carbon on the surface of 0.5Na/4Ag/4ZrO_2/SBA-16 over 4Ag/4ZrO_2/SBA-16 (6.64% total carbon vs. 5.54%, respectively). A higher coking formation rate over 0.5Na/4Ag/4ZrO_2/SBA-16 is not surprising because its selectivity to butadiene coke precursor is higher (e.g., 62% compared to 50% for the baseline catalyst, TOS = 72 hr). While the conversion decreases more significantly for the 0.5Na/4Ag/4ZrO_2/SBA-16 catalyst, its butadiene yield remains higher (i.e., 28.6% vs. 24.9% for 4Ag/4ZrO_2/SBA-16) after 72 hr TOS. Figure 5 shows the evolution of the ratio acetaldehyde + butadiene + butenes (dehydrogenation pathway) over ethylene + DEE (dehydration pathway) for both catalysts. As expected, the ratio is over 1 for both catalysts during 72 hr TOS, and as such, the dehydrogenation pathway is the most favored pathway for both catalysts. The decrease of the ratio with TOS indicates that the dehydration pathway becomes more favorable (but not predominant) with TOS. This may be due to sintering of Ag and/or selective coking of the acid sites responsible for butadiene formation.

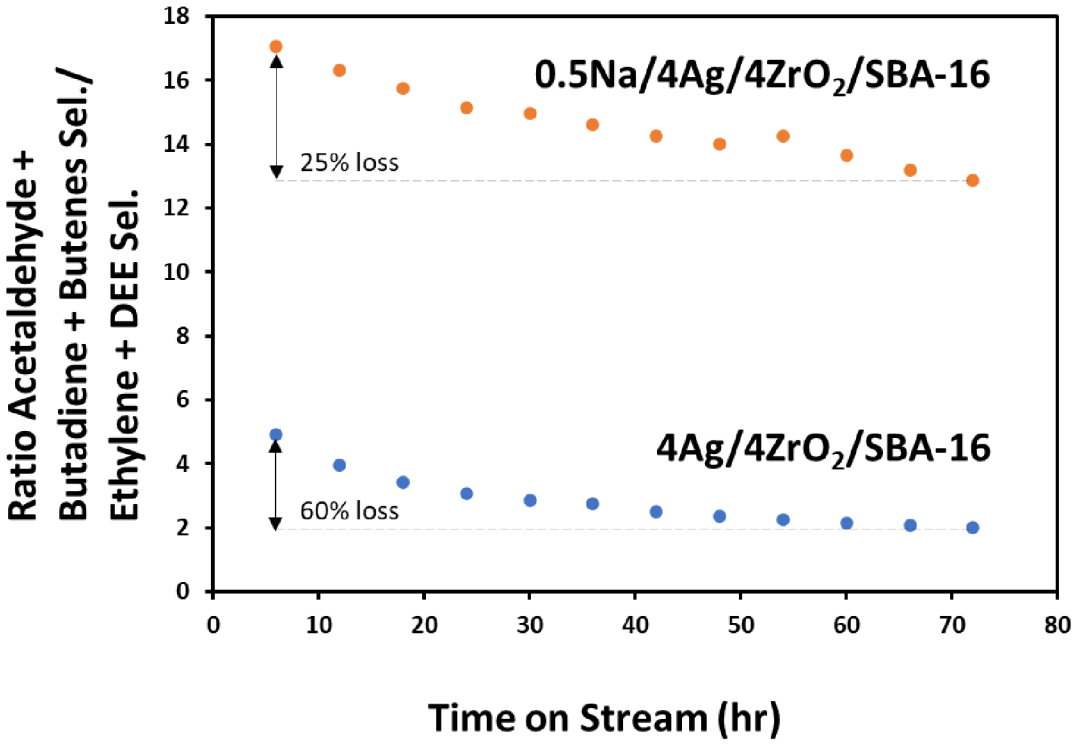

Figure 5. Evolution of the ratio (acetaldehyde + butadiene + butene)/(ethylene + diethyl ether) with TOS for 0.5Na/4Ag/4ZrO_2/SBA-16 and 4Ag/4ZrO_2/SBA-16 from reactivity measurements presented in Figure 4.

Interestingly, the loss of activity for the dehydrogenation pathway is more predominant with the 4Ag/4ZrO_2/SBA-16 catalyst for which the dehydrogenation pathway products/dehydration pathway product ratio decreases by 60% after 72 hr TOS as compared to only 25% for the 0.5Na/4Ag/4ZrO_2/SBA-16 catalyst. This activity loss could be because the initial ratios (at TOS = 5 hr) are different for both catalysts. Alternatively, it could be because 1) Na limits sintering of Ag by encapsulating the particles and/or 2) coking is "selective" over the 0.5Na/4Ag/4ZrO_2/SBA-16 catalyst and appears to be more predominant on the acid sites active for ethanol dehydration as compared to acetaldehyde condensation. To check these hypotheses, the Ag particle size of the fresh catalysts and spent samples were determined from the XRD patterns and TEM analysis. The results presented in Table 3 shows that the Ag particle size increases more significantly for the

4Ag/4ZrO_2/SBA-16 catalyst as compared with the 0.5Na/4Ag/4ZrO_2/SBA-16 catalyst. This result confirms that Na promotes resistance to Ag metal sintering during reaction.

Table 3. Approximate Ag particle size from the XRD patterns and average particle size from TEM images of the fresh and spent catalysts from the 72 hr lifetime studies presented in Figure 4.

Catalyst	Ag Particle Size (nm)	
	XRD	TEM
Fresh 4Ag/4ZrO2/SBA-16	3.4	2.7
Spent 4Ag/4ZrO2/SBA-16	4	3.9
Fresh 0.5Na/4Ag/4ZrO2/SBA-16	2.6	1.9
Spent 0.5Na/4Ag/4ZrO2/SBA-16	2.9	2.5

Acidy measurements before and after exposure to ethanol at 325°C also were conducted, and the FTIR spectra obtained after pyridine desorption at 150°C are presented in Figure 6 for the 0.5Na/4Ag/4ZrO_2/SBA-16 catalysts. Similar spectra were obtained for the 4Ag/4ZrO_2/SBA-16 catalyst. Ethanol exposure of the catalyst pellet approximately corresponds to the state of the catalyst at 22hr TOS under the reaction conditions shown in Figure 4. The concentration of the acid sites for each catalyst before and after ethanol exposure are shown in Table 4. While both catalysts suffer from a decrease of acid site concentrations after exposure to ethanol, the loss is more drastic for the 0.5Na/4Ag/4ZrO_2/SBA-16 catalyst. Additionally, for this catalyst, the results suggest that the weaker acid sites are the ones that are poisoned from coking after exposure to ethanol. Thus, the results support the hypothesis according to which coking of the acid sites is more selective over the 0.5Na/4Ag/4ZrO_2/SBA-16 catalyst. It is possible that ethanol dehydration to ethylene and DEE is more facile over the weaker acid site compared to acetaldehyde condensation. A such, a selective decrease of the concentration of the weaker acid site could slow

down the decrease of the (acetaldehyde + butadiene + butenes)/ (ethylene + DEE) ratio with TOS. Therefore, the superior loss of activity for the dehydrogenation pathway observed with the baseline after 72 hr TOS as compared to the 0.5Na/4Ag/4ZrO_2/SBA-16 catalyst may be due to the fact that during reaction, Na limits sintering of Ag particles and promotes selective coking of the acid sites.

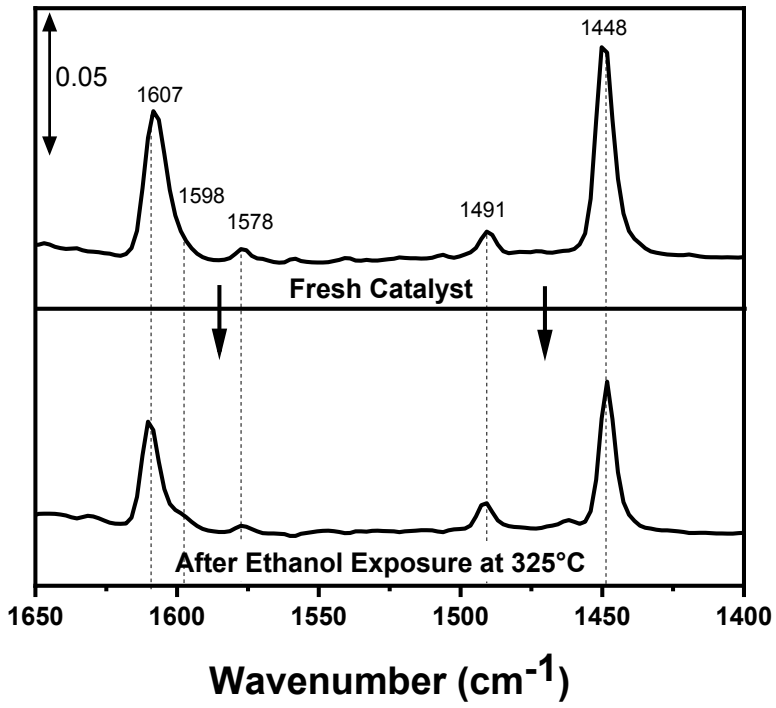

Figure 6. Infrared spectra recorded after pyridine adsorption at 50°C followed by desorption at 150°C for the 0.5Na/4Ag/4ZrO_2/SBA-16 baseline catalyst before and after exposure to ethanol at 325°C. The baseline spectra recorded prior to pyridine or ethanol adsorption were subtracted from the ones obtained after pyridine desorption at 150°C and ethanol adsorption. Spectra were normalized to a pellet of 20 mg and 2 cm^2. Py-L at 1448 cm^{-1} was used for quantification.

Table 4. Effect of ethanol exposure at 325°C on catalyst acidity over (0.5Na)/4Ag/4ZrO_2/SBA-16 catalysts

Catalyst	Lewis Acid Site Concentration (μmol/g)			
	Weak	Medium	Strong	Total
4Ag/4ZrO_2/SBA-16				
Fresh Catalyst	35.1	7.2	1.1	43.4
Post Ethanol Exposure	30.5	7.0	0	37.5
0.5Na/4Ag/4ZrO_2/SBA-16				
Fresh Catalyst	20.6	3.4	1.4	25.5

Post Ethanol Exposure	12.7	1.9	1.7	16.3

4. Conclusions

In this work, we investigated the effects of adding Na and K to 4Ag/4ZrO_2/SBA-16 catalyst on the catalytic performance for single-bed conversion of ethanol to butadiene. Addition of 0.5% Na or 0.5% K to 4Ag/4ZrO_2/SBA-16 leads to a 10% loss in conversion from about 96% to 87-89% when operating under mild conditions (T =325°C, P = 1 atmosphere, WHSV= 0.23 hr^{-1}, TOS = 5 hr). However, adding Na or K is beneficial because the butadiene selectivity and productivity are improved. Indeed, a 50% increase in butadiene productivity was observed for the 0.5Na/4Ag/4ZrO_2/SBA-16 catalyst. A remarkable butadiene selectivity of 75% was achieved while maintaining high conversion (i.e., 90%) with the 0.5Na/4Ag/4ZrO_2/SBA-16 catalyst. Characterization of the fresh catalysts indicated that the concentration of the Lewis acid sites and the Ag particle size were both decreased with Na or K addition to the catalyst. This change in catalyst properties is advantageous because it leads to a decrease in the undesirable ethanol dehydration reaction, which competes with the desirable ethanol dehydrogenation reaction. Catalyst stability was examined for the preferred 0.5Na/4Ag/4ZrO_2/SBA-16 catalyst compared with the baseline 4Ag/4ZrO_2/SBA-16 catalyst. We found that the conversion loss is more significant for 0.5Na/4Ag/4ZrO_2/SBA-16 and equal to 55% (after 72 hr TOS) as compared to a 45% decrease for 4Ag/4ZrO_2/SBA-16. This is attributed to the fact that butadiene formation is higher with the Na addition, resulting in a higher coking rate from butadiene polymerization. While a higher deactivation rate was observed with 0.5Na/4Ag/4ZrO_2/SBA-16, butadiene productivity was still higher when Na was added, with this benefit existing through the entire study period.

CRediT authorship contribution statement

Austin Winkelman: Catalyst synthesis, testing, and characterization, methodology, conceptualization, data analysis, interpretation of results, and writing the manuscript. **Vanessa Lebarbier Dagle:** Supervision and experimental direction, conceptualization, interpretation of results, manuscript writing and reviewing. **Teresa Lemmon:** LC data collection and analysis from activity tests. **Libor Kovarik:** TEM data acquisition and assistance in interpretation. **Yong Wang:** Supervision, data interpretation, reviewing the manuscript. **Robert Dagle:** Supervision, data interpretation, reviewing of the manuscript.

Declaration of Competing Interest

The authors declare that they have no known competing financial interests or personal relationships that could have appeared to influence the work reported in this paper.

Acknowledgements

This work was funded by the U.S. Department of Energy (DOE) Bioenergy Technologies office and performed at Pacific Northwest National Laboratory (PNNL) under contract DE-AC05-76RL01830. Catalyst characterization equipment use was granted by a user proposal at the William R. Wiley Environmental Molecular Sciences Laboratory, which is a national scientific user facility sponsored by the DOE Office of Biological and Environmental Research and located at PNNL. This work as also supported in part through the PNNL-Washington State University Distinguished Graduate Research Program for A.D.W. The authors wish to acknowledge Tom Wietsma for his help with total carbon measurements.

The views and opinions of the authors expressed herein do not necessarily state or reflect those of the U.S government or any agency thereof or any of their employees, makes any warranty, expressed or implied, or assumes any legal liability or responsibility for the accuracy,

completeness, or usefulness of any information, apparatus, or process disclosed, or represents that its use would not infringe privately owned rights.

References

1. Global Butadiene Market 2020: Industry Trends and Investigation Growth Rate, Consumption by Regional data, Product & Application Segmentation, Key Companies Showing Impressive Growth by 2026 [press release]. MarketWatch, August 24 2020.

2. Butadiene Market to Reach USD 23.49 Billion by 2027 | Reports and Data [press release]. GlobeNewswire, March 25 2020.

3. White WC. Butadiene production process overview. Chem Biol Interact. 2007;166(1-3):10-4.

4. Dagle RA, Winkelman AD, Ramasamy KK, Lebarbier Dagle V, Weber RS. Ethanol as a Renewable Building Block for Fuels and Chemicals. Industrial & Engineering Chemistry Research. 2020;59(11):4843-53.

5. Annual Fuel Ethanol Production: U.S. and world Ethanol Production. 2020.

6. Lebedev S. British Patent 331402, 1929.(b) Lebedev, S. V. British Patent. 1930;331482.

7. Ostromislenskiy J. Production of butadiene. J Russ Phys Chem Soc. 1915;47:1472-506.

8. Pomalaza G, Capron M, Ordomsky V, Dumeignil F. Recent Breakthroughs in the Conversion of Ethanol to Butadiene. Catalysts. 2016;6(12):203.

9. Sun J, Wang Y. Recent Advances in Catalytic Conversion of Ethanol to Chemicals. ACS Catalysis. 2014;4(4):1078-90.

10. Dagle VL, Flake MD, Lemmon TL, Lopez JS, Kovarik L, Dagle RA. Effect of the SiO2 support on the catalytic performance of Ag/ZrO2/SiO2 catalysts for the single-bed production of butadiene from ethanol. Appl Catal B-Environ. 2018;236:576-87.

11. Sushkevich VL, Ivanova II, Taarning E. Mechanistic Study of Ethanol Dehydrogenation over Silica-Supported Silver. ChemCatChem. 2013;5(8):2367-73.

12. Sushkevich VL, Ivanova, II, Ordomsky VV, Taarning E. Design of a metal-promoted oxide catalyst for the selective synthesis of butadiene from ethanol. ChemSusChem. 2014;7(9):2527-36.

13. Sushkevich VL, Ivanova II, Taarning E. Ethanol conversion into butadiene over Zr-containing molecular sieves doped with silver. Green Chemistry. 2015;17(4):2552-9.

14. Sushkevich VL, Ivanova II. Mechanistic study of ethanol conversion into butadiene over silver promoted zirconia catalysts. Applied Catalysis B: Environmental. 2017;215:36-49.

15. Makshina EV, Dusselier M, Janssens W, Degreve J, Jacobs PA, Sels BF. Review of old chemistry and new catalytic advances in the on-purpose synthesis of butadiene. Chem Soc Rev. 2014;43(22):7917-53.

16. Emeis CA. Determination of Integrated Molar Extinction Coefficients for Infrared Absorption Bands of Pyridine Adsorbed on Solid Acid Catalysts. Journal of Catalysis. 1993;141(2):347-54.

17. Da Ros SJ, Matthew D.; Mattia, Davide; Pinto, Jose; Schwaab, Marcio; Noronha, Fabio B.; Kondrat, Simon A.; Clarke, Tomos C.; Taylor, Stuart H. Ethanol to 1,3-butadiene conversion using ZrZn-containing MgO-SiO2 systems prepared by co-precipitation and effect of catalyst acidity modification. ChemCatChem. 2016;8(14):2376-86.

18. Patil PT, Liu D, Liu Y, Chang J, Borgna A. Improving 1,3-butadiene yield by Cs promotion in ethanol conversion. Applied Catalysis A: General. 2017;543:67-74.

19. Baylon RAL, Sun J, Wang Y. Conversion of ethanol to 1,3-butadiene over Na doped Zn Zr O mixed metal oxides. Catalysis Today. 2016;259:446-52.

20. Winiarek P, Kijeński J. Hydrogenation of unsaturated hydrocarbons over alkali-metal-modified zinc oxide. Journal of the Chemical Society, Faraday Transactions. 1998;94(1):167-72.

21. Qin R, Zhou L, Liu P, Gong Y, Liu K, Xu C, et al. Alkali ions secure hydrides for catalytic hydrogenation. Nature Catalysis. 2020;3(9):703-9.

22. Dagle V, Winkelman AD, Jaegers NR, Saavedra-Lopez J, Hu JZ, Engelhard MH, et al. Single-step conversion of ethanol to n-butenes over Ag-ZrO2/SiO2 catalysts. ACS Catalysis. 2020.

23. Akhade SA, Winkelman A, Lebarbier Dagle V, Kovarik L, Yuk SF, Lee M-S, et al. Influence of Ag metal dispersion on the thermal conversion of ethanol to butadiene over Ag-ZrO2/SiO2 catalysts. Journal of Catalysis. 2020;386:30-8.

24. Ezinkwo GO, Tretyakov VP, Aliyu A, Ilolov AM. Fundamental Issues of Catalytic Conversion of Bio-Ethanol into Butadiene. ChemBioEng reviews. 2014;1(5):194-203.